Particle-hole configurations in reaction mechanisms for single-particle level densities for target nuclei in (n,p) reactions at 14.8 MeV energy

H. S. Hans,* A. Kumar,† Shivcharan Verma, Gulzar Singh, B. R. Behera, and K. P. Singh
Department of Physics, Panjab University, Chandigarh, India

Sudip Ghosh
Saha Institute of Nuclear Physics, Calcutta, India

(Received 29 September 2014; published 24 September 2015)

Earlier, single-particle level densities were obtained for a large number of target nuclei from the analysis of experimental data on a (n,p) reaction at 14.8 MeV neutron energy using the Kalbach model. Recently, we obtained theoretical values of excitation energy ε_c for unbound states and Fermi energies (ε_f) for bound states for these single-particle level densities for many target nuclei by using Shlomo's theory, which leads to a shell structure, when ε_c was plotted as a function of the atomic weight A. This indicates support to the concept of multiple statistical direct (MSD) and multiple statistical compound preequilibrium processes that involves unbound and bound states. We have now calculated the particle-hole configurations which are dominantly involved in the reaction mechanism for creating the single-particle level densities for all target nuclei, including "spikes" and "dips" obtained in the data analysis earlier using the formulation given by Kalbach [Phys. Rev. C **23**, 124 (1981)] and Shlomo [Nucl. Phys. A **539**, 17 (1992)]. It seems that $h = 2$, $p = 0$ is the dominant configuration for most of the targets in the preequilibrium process, whereas spikes seem to correspond to the $h = 1$, $p = 1$ dominant configuration, corresponding to the direct reaction mechanism; and dips seem to belong to the $h = 2$, $p = 0$ configuration and $h = 1$, $p = 1$ and $h = 0$, $p = 2$ configurations somewhat equally giving compound nucleus formation due to quantum statistical fluctuations and MSD. The implication of these calculations and results is discussed.

DOI: 10.1103/PhysRevC.92.034614 PACS number(s): 21.10.Ma, 24.60.Dr, 25.40.Kv

I. INTRODUCTION

We had analyzed [1] the global data on angle integrated energy spectra and energy integrated angular distribution of protons from the (n,p) reaction at 14.8 MeV of neutron energy for a large number of target nuclei to obtain single-particle level densities by using the PRECO-D2 computer program by Kalbach [2] which uses the assumption of the preequilibrium process as well as the compound nucleus formation. The target-projectile composite nuclear system is assumed to reach compound nucleus equilibrium through a cascade of two-body interactions. Each stage of the cascade is characterized by the number of excited particles (p) and holes (h), called excitons. Kalbach uses a semiclassical model of multiple statistical direct (MSD) and multiple statistical compound (MSC) processes based on the Feshbach-Kerman-Koonin [3] quantum-mechanical theory of preequilibrium reactions which results in the emission of a particle leaving behind an excited nucleus through the multistep direct (MSD) process, which decays further through the multistep compound (MSC) process. The compound state is thus reached through MSD-MSC transition, which also includes the evaporation model of Weisskopf and Ewing [4]. The Kalbach model also includes a direct reaction, not included in MSD. These are nucleon transfer and nucleon knockout, and they are evaluated semiempirically [2].

It was interesting [5] to find that the excitation energies ε_c of the single-particle level densities calculated by using Shlomo's model [6] of energy dependence of the single-particle level densities obtained from comparison of experimental data with the Kalbach model had a shell structure when ε_c was plotted against the atomic weight of target nuclei A. The values of ε_c for closed shell target nuclei, such as ${}_{20}\mathrm{Ca}^{40}$ $(n = p = 20)$ and ${}_{28}\mathrm{Ni}^{58}$ $(p = 28)$ and ${}_{39}\mathrm{Y}^{89}$ $(n = 50)$ had low values of ε_c, i.e., 47.3, 47.5, and 40 MeV compared to 51–57.0 MeV for other targets, which had proton and neutron values different from magic numbers. This showed a certain systemization of the process of excitation in the preequilibrium model. This is clearly shown in Fig. 7 of Ref. [5].

It was also seen that the semiempirical values of g_c^{Th} corresponded to the negative energy of excitation ε_B, which when plotted against A (atomic weight) of the target nuclei had also a shell structure but with a higher value of ε_B at a magic number and lower values at nonmagic numbers. This is, thus complementary to the dependence of ε_c on A and is shown in Fig. 6 of Ref. [5].

It seems that the values of ε_c, which correspond to the unbound states, represent the MSD process in Fig. 7 of Ref. [5], and ε_B, which corresponds to bound states, represents the MSC process (Fig. 6, Ref. [5]). On the other hand, Fermi energies ε_f when plotted against A had no structure. They, in general, went down with A (Fig. 8, Ref. [5])

It is pertinent to ask if there is any systematics involving particle-hole configuration in the reaction mechanism of the multistep processes of MSD, MSC, and Fermi excitation energies in the involvement of the (p,h) process.

We found that Eq. (13) of the Kalbach model can answer this question if we interpret appropriately the quantities in this equation with respect to the ones we have used in Ref. [1].

*Deceased on 19th March, 2014.
†Corresponding author: ashok@pu.ac.in

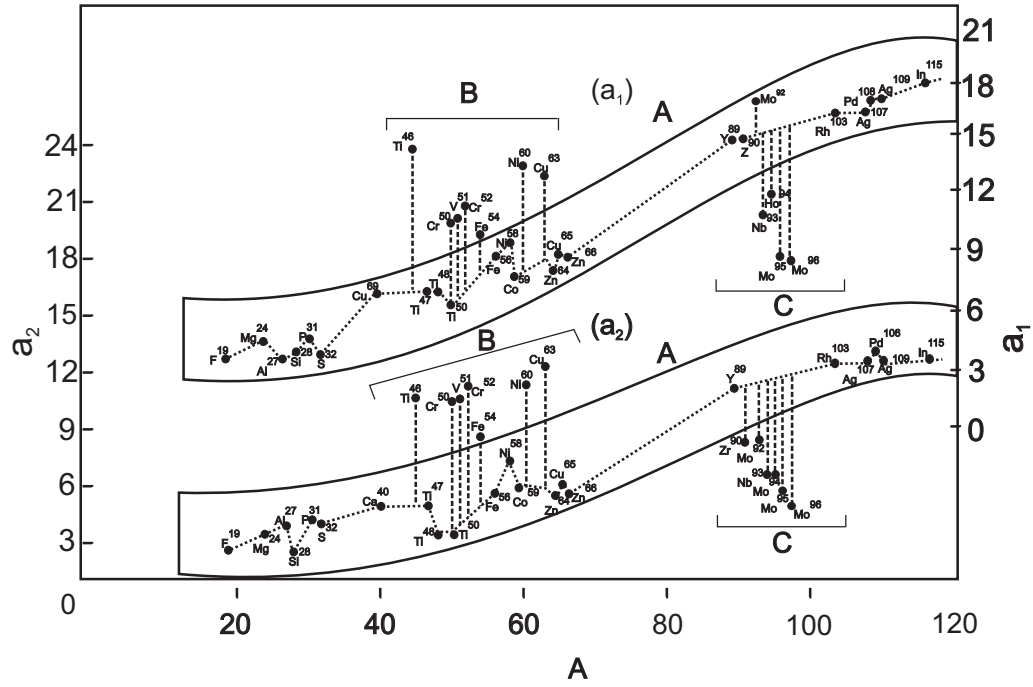

FIG. 1. The values of $a_1 = \frac{\pi^2 g_c}{6}$ and $a_2 = \frac{\pi^2 g_R}{6}$ as a function of atomic weight as derived from the comparison of the experimental data with the Kalbach model [2]. *A* corresponds to the smooth part, *B* corresponds to spikes, and *C* corresponds to dips.

Then

$$g_u(p) = g_o\left[\frac{p-1}{n-1}\left(\frac{V+\left(\frac{E-S}{n}\right)}{V}\right)^{\frac{1}{2}} + \frac{h}{n-1}\left(\frac{V-\left(\frac{E-S}{n}\right)}{V}\right)^{\frac{1}{2}}\right] \quad \text{for } h \leqslant 2, \tag{1}$$

where $g_u(p) = g_c(\text{exp})$ and $g_o = g_R(\text{exp})$ and $h =$ the number of holes involved in the reaction, $p =$ the number of particles involved in the reaction, and

$$n = h + p = 2. \tag{2}$$

Also $E = \langle \varepsilon_c \rangle$, $S = (\varepsilon_f)$, and

$$V = -\langle V_0 \rangle = -\left(\frac{V_0 n + V_0 p}{2}\right). \tag{3}$$

In this manner we can write Eq. (1) as

$$g_c(\text{exp}) = g_R(\text{exp})\left[\frac{p-1}{n-1}\left(\frac{-\langle V_o\rangle + \left(\frac{\langle \varepsilon_c\rangle - (\varepsilon_f)}{2}\right)}{-\langle V_o\rangle}\right)^{1/2} + \frac{h}{n-1}\left(\frac{-\langle V_o\rangle - \left(\frac{\langle \varepsilon_c\rangle - (\varepsilon_f)}{2}\right)}{-\langle V_o\rangle}\right)^{1/2}\right]. \tag{4}$$

Equation (4) is expected to reproduce the proper values of particles (p) and holes (h), which are involved in the process, which gives rise to $g_c(\text{exp})$ and $g_R(\text{exp})$ in the Kalbach model. The values of various quantities, i.e., $g_c(\text{exp})$, $g_R(\text{exp})$, and $\langle \varepsilon_c \rangle$, (ε_f) used in Eq. (4) have been obtained as a result of three major operations discussed below:

(i) The experimental data of the energy spectra and the angular distribution of protons in the (n,p) reaction at 14.8 MeV neutron energy as given in several papers, published over several years from 1959 to 1988, as discussed in Ref. [1] is used for comparison with the Kalbach model using the PRECO-D2 computer program.

(ii) The evaluation of $g_c(\text{exp})$ and $g_R(\text{exp})$ is carried out by fitting the experimental data with the Kalbach model by a trial and error method.

(iii) The values of $g_c(\text{exp})$ and $g_R(\text{exp})$ for 23 target nuclei are fitted to Shlomo's model of dependence of the single-particle level densities on the energy of excitation $\langle \varepsilon_c \rangle$.

Now in this paper, we are trying to correlate the reaction mechanism, i.e., involvement of particles (p) and holes (h) in the preequilibrium processes in trying to find out the dominance of any configuration, i.e., (i) $h = 2$, $p = 0$, and $n = 2$, (ii) $h = 1$, $p = 1$, and $n = 2$, and (iii) $h = 0$, $p = 2$, and $n = 2$ in a given process.

We have compared the relationship of $\frac{g_c\ (\text{exp})}{g_R\ (\text{exp})}$ with the values of Eq. (4) using the values of $\langle \varepsilon_c \rangle$ and (ε_f) of Ref. [6] for three ranges of nuclei:

(i) First we have examined 23 cases of nuclei for which the values of $g_c(\text{exp})$ and $g_R(\text{exp})$ lie on a smooth curve as shown in Fig. 1. As discussed in Ref. [1], this region extends over a wide range of nuclei from $A = 19$ to $A = 115$, marked as *A* in Fig. 1.

(ii) Next we have discussed the range of seven nuclei, i.e., $46 < A < 63$, for which the values of both $g_c(\text{exp})$ and $g_R(\text{exp})$ are much higher than required by the general smooth trend of the relation of g versus A. We have marked these nuclei as "*B*" in Fig. 1. The values

of g_c(exp) and g_R(exp) in these cases are termed as spikes.

(iii) Then we found another region of six nuclei on the higher side of the atomic weight, i.e., $90 < A < 96$ for which both g_c(exp) and g_R(exp) are quite low. These are dips. We have marked these nuclei as "*C*" in Fig. 1.

The characteristics obtained by the use of the relationship of Eq. (4) are quite different in three cases, which will be discussed below.

II. RESULTS AND DISCUSSION

We give below the results of our calculations for these three regions:

A.

For the first category of 23 target nuclei marked as *A* in Fig. 1, the values of g_c(exp) and g_R(exp) are determined by the procedure laid out in Ref. [1] where the Kalbach model is used to compare, by a trial and error method, the experimental result of energy spectra and angular distribution of the world data of (n,p) reactions at 14.8 MeV neutron energy through the PRECO-D2 computer code. These values are given in Table I of Ref. [5] and are given in Table Ia in the present paper.

The values of $\langle\varepsilon_c\rangle$ and (ε_f), i.e., the excitation energies for the unbound states and the Fermi energy for the bound states are, on the other hand, determined by using Shlomo's model, following the procedure in Ref. [5] and are given in Tables VI and VII in that reference. It is interesting to see from Fig. 7 of Ref. [5] that the values of $\langle\varepsilon_c\rangle$ for g_c(exp) have a shell structure when plotted against A.

We are now giving, for 23 target nuclei, in Table Ia of this paper, the values of $\langle\varepsilon_c\rangle$,$(\varepsilon_f)$, $g_c(\text{exp}) = g_u(p)$, $g_R(\text{exp}) = g_o$ and $R_{\text{exp}} = \frac{g_u(p)}{g_0} = \frac{g_c(\text{exp})}{g_R(\text{exp})}$, and the values of the ratio R_{Th} as given on the right side of Eq. (4) for three conditions of the particle hole (p,h) configuration, i.e., for: (i) $h = 2$, $p = 0$, (ii) $h = 1$, $p = 1$, and (iii) $h = 0$, $p = 2$ for $n = 2$ as calculated from the Kalbach model and Shlomo's model.

In Table Ib, we have given values of $f_i = \frac{R_{Th}}{R_{\text{exp}}}$, $\frac{\Delta_i}{R_{\text{exp}}} = \frac{1-f_i}{R_{\text{exp}}}$, and $(\frac{\Delta_1}{\Delta_i})^2$ in three columns for $i = 1$, $i = 2$, and $i = 3$ for a set of eight target nuclei, which have even-even structure. In Tables Ic and Id, we have given these values for the rest of the 15 nuclei, which are even-odd, odd-odd, and even-even.

It is interesting to observe that the values of $(\frac{\Delta_1}{\Delta_i})^2$ for eight even-even target nuclei as given in Table Ib, i.e., $_{12}Mg^{24}$, $_{14}Si^{28}$, $_{20}Ca^{40}$, $_{22}Ti^{50}$, $_{26}Fe^{56}$, $_{30}Zn^{64}$, and $_{30}Zn^{66}$ for $i = 2$ and $i = 3$ are quite small when we take the value of $(\frac{\Delta_1}{\Delta_i})^2$ for $i = 1$ as 1.00. They range from 0.09 to 0.19 for $i = 2$ which corresponds to the $h = 1$, $p = 1$ configuration and range from 0.014 to 0.068 for $i = 3$, which corresponds to the $h = 0$, $p = 2$, configuration. This shows that $i = 1$ which corresponds to the $h = 2$, $p = 0$ configuration is the most dominant configuration. We have taken $i = 1$ as the reference value because it corresponds to the smallest set of values of $\frac{\Delta_i}{R_{\text{exp}}}$, the average value of which is 0.005 for $i = 1$, compared to 0.17 for $i = 2$ and 0.32 for $i = 3$. We have further given in Tables Ic and Id, the values of $(\frac{\Delta_1}{\Delta_i})^2$ for $i = 2$ and $i = 3$

TABLE Ia. The values of $\langle\varepsilon_c\rangle = E$, $(\varepsilon_f) = S$, $\langle V_0\rangle$, $g_c(\text{exp}) = g_u(p)$, $g_R(\text{exp}) = g_o$, $\frac{g_c\ (\text{exp})}{g_R\ (\text{exp})} = R(\text{exp})$, and $R(Th)$ [as given in Eq. (4)] for all the target nuclei.

No.	Nucleus	$\langle\varepsilon_c\rangle = E$	$\langle\varepsilon_f\rangle = S$	$\langle V_0\rangle$	$g_c(\text{exp}) = g_u(p)$	$g_R(\text{exp}) = g_0$	$\frac{g_c(\text{exp})}{g_R(\text{exp})} = R(\text{exp})$	R_{Th}(p,h) configuration		
								$h = 2\ p = 0$	$h = 1\ p = 1$	$h = 0\ p = 2$
1	$_9F^{19}$	48.6	34.54	43.45	2.49	1.5	1.6	1.153	1.06	0.85
2	$_{12}Mg^{24}$	51.6	32.96	43.30	2.78	2.01	1.38	1.31	1.1	0.88
3	$_{13}Al^{27}$	52.9	34.02	42.6	2.87	2.37	1.21	1.32	1.1	0.88
4	$_{14}Si^{28}$	57.3	32.05	42.5	2.49	1.52	1.63	1.85	1.36	0.84
5	$_{15}P^{31}$	57.6	34.14	42.8	2.89	2.49	1.15	1.34	1.1	0.86
6	$_{16}S^{32}$	57.05	33.18	42.2	2.49	2.43	1.025	1.47	1.16	0.85
7	$_{20}Ca^{40}$	47.3	33.14	41.8	4.5	2.98	1.49	1.49	1.23	0.97
8	$_{22}Ti^{47}$	50.4	33.22	41.6	4.5	2.01	2.2	1.2	1.09	0.90
9	$_{22}Ti^{48}$	56.00	31.99	41.2	4.07	2.01	2.2	1.3	1.13	0.85
10	$_{22}Ti^{50}$	56.50	32.28	41.0	4.07	2.98	1.48	1.45	1.17	0.85
11	$_{26}Fe^{56}$	51.00	32.23	41.8	5.47	4.01	1.3	1.3	1.1	0.89
12	$_{27}Co^{59}$	56.2	33.32	41.2	4.99	4.01	1.24	1.36	1.11	0.91
13	$_{28}Ni^{58}$	47.50	32.25	41.0	6.02	4.50	1.33	1.33	1.1	0.90
14	$_{29}Cu^{65}$	55.8	33.78	41.0	5.47	2.98	1.83	1.32	1.10	0.88
15	$_{30}Zn^{64}$	55.7	33.12	40.9	4.99	2.98	1.64	1.47	1.0	0.85
16	$_{30}Zn^{66}$	57.7	33.02	42.59	5.47	4.01	1.33	1.37	1.11	0.85
17	$_{39}Y^{89}$	40.2	32.97	40.2	9.00	6.50	1.37	1.12	1.04	0.97
18	$_{45}Rh^{103}$	39.80	32.86	39.7	10.3	7.54	1.36	1.13	1.04	0.95
19	$_{46}Pd^{106}$	39.71	31.96	39.7	11.00	7.53	1.45	1.2	1.04	0.96
20	$_{46}Pd^{108}$	43.40	31.81	39.6	10.40	7.54	1.31	1.11	1.07	0.93
21	$_{47}Ag^{107}$	43.40	32.77	39.6	10.09	7.93	1.4	1.36	1.12	0.88
22	$_{47}Ag^{109}$	43.7	32.66	39.6	10.52	7.56	1.39	1.16	1.06	0.96
23	$_{49}In^{115}$	43.4	32.36	39.9	11.00	7.93	1.38	1.23	1.11	0.99

TABLE Ib. The values of $f_i = \frac{R_{TH}}{R_{\exp}}$, $\frac{\Delta_i}{R_{\exp}} = \frac{1-f_1}{R_{\exp}}$, and $(\frac{\Delta_1}{\Delta_i})^2$ for three configurations $i = 1$, $i = 2$, and $i = 3$ for eight even-even nuclei.

No.	Nucleus	$f_i = \frac{R_{Th}}{R_{\exp}}$			$\frac{\Delta_i}{R_{\exp}} = \frac{1-f_i}{R_{\exp}}$			$(\frac{\Delta_1}{\Delta_i})^2$		
		$i=1$	$i=2$	$i=3$	$i=1$	$i=2$	$i=3$	$i=1$	$i=2$	$i=3$
1	$_{12}Mg^{24}$	0.95	0.83	0.58	0.036	0.12	0.305	1.00	0.090	0.014
2	$_{14}Si^{28}$	1.1	0.77	0.53	0.061	0.14	0.28	1.00	0.190	0.040
3	$_{20}Ca^{40}$	1.00	0.81	0.50	0.00	0.22	0.31	1.00	0.000	0.000
4	$_{22}Ti^{50}$	0.86	0.88	0.50	0.071	0.22	0.31	1.00	0.090	0.050
5	$_{26}Fe^{56}$	1.00	0.83	0.74	0.00	0.13	0.20	1.00	0.000	0.000
6	$_{28}Ni^{58}$	1.00	0.68	0.66	0.00	0.13	0.22	1.00	0.000	0.000
7	$_{30}Zn^{64}$	0.87	0.66	0.50	−0.09	0.19	0.34	1.00	0.190	0.068
8	$_{30}Zn^{66}$	1.05	0.83	0.69	−0.037	0.12	0.26	1.00	0.110	0.019
Averages		0.96	0.78	0.59	0.005	0.17	0.32	1.00	0.020	0.024

for nuclei, which are odd-even, odd-odd, and even-even, along with values for $(\frac{\Delta_1}{\Delta_i})^2$ for $i = 1$. It is interesting to find that the values of $(\frac{\Delta_1}{\Delta_i})^2$ for these cases are much larger than for the eight even-even nuclei for $i = 2$ and $i = 3$. They range from 0.24 to 0.82 for $i = 2$ and from 0.16 to 0.64 for $i = 3$ compared to 0.09 to 0.19 for $i = 2$ and 0.014 to 0.068 for $i = 3$ for the eight even-even target nuclei, but they are still less than 1 for the nuclei in Table Ic. The values of $(\frac{\Delta_1}{\Delta_i})^2$ for the nuclei in Table Id do not seem to fit in any systematics given above, perhaps due to some nuclear structure effects.

All these results, put together, show very clearly that for nuclei, involving the preequilibrium process on the main curve A, the dominant configuration of the reaction is $h = 2$, $p = 0$ $(i = 1)$.

We have plotted in Fig. 2, the values of $\frac{\Delta_i}{R_{\exp}}$ as a function of atomic weight A for the three possible configurations of particle-hole (p,h) in the process of the nuclear reaction for 23 targets designated under category A of Fig. 1, i.e., for:

(i) $h = 2$, $p = 0$, and $n = 2$;
(ii) $h = 1$, $p = 1$, and $n = 2$, and
(iii) $h = 0$, $p = 2$, and $n = 2$.

It is quite apparent from Fig. 2 that the values $\frac{\Delta_i}{R_{\exp}}$ have the least spread in Fig. 2(a) with the $h = 2$, $p = 0$, configuration for the eight even-even nuclei. It shows that this configuration is most probable in the reaction mechanism. It is quite interesting to see that for nuclei with magic proton or neutron numbers, this value is "zero," e.g., for $_{20}Ca^{40}_{20}$ and $_{28}Ni^{58}_{30}$. For many other near magic nuclei, such as $_{12}Mg^{24}$, $_{14}Si^{28}$, $_{22}Ti^{50}$, $_{26}Fe^{56}$, $_{30}Zn^{64}$, and $_{30}Zn^{66}$ the values of $\frac{\Delta_i}{R_{\exp}}$ are quite near to zero.

For these eight even-even nuclei, the average value of $\frac{\Delta_i}{R_{\exp}}$ in the $h = 2$, $p = 0$ $(i = 1)$ configuration is 0.005 as shown in Fig. 2(a) and Table Ib, compared to 0.13 for the 11 even-odd target nuclei in Fig. 2(b) and Table Ic. On the other hand for $i = 2$ the average value of $\frac{\Delta_i}{R_{\exp}}$ is 0.17, and for $i = 3$ it is 0.32 as shown in Table Ib for 8 even-even nuclei whereas it is 0.18 for $i = 2$ and 0.23 for $i = 3$ for the case for the 11 even-odd target nuclei shown in Table Ic. The four nuclei in Table Id, i.e., $_{13}Al^{27}$, $_{15}P^{31}$, $_{16}S^{32}$, and $_{27}Co^{59}$ seem to represent the effect of nuclear structure on the values of $\frac{\Delta_i}{R_{\exp}} = \frac{1-f_i}{R_{\exp}}$. Whereas in Table Ic, the values of $\frac{\Delta_i}{R_{\exp}}$ for $i = 1$ represent minimum values compared to $i = 2$ and $i = 3$, but the nuclei shown in Table Id seem to show this minimum for $i = 2$. This ends up giving $(\frac{\Delta_1}{\Delta_i})^2$ no systematics when we take $(\frac{\Delta_1}{\Delta_i})^2 = 1$ for $i = 1$, but

TABLE Ic. The values of $f_i = \frac{R_{Th}}{R_{\exp}}$, $\frac{\Delta_i}{R_{\exp}} = \frac{1-f_i}{R_{\exp}}$, and $(\frac{\Delta_1}{\Delta_i})^2$ for the group of target nuclei (even-odd, odd-odd, and even-even).

No.	Nucleus	$f_i = \frac{R_{Th}}{R_{\exp}}$			$\frac{\Delta_i}{R_{\exp}} = \frac{1-f_i}{R_{\exp}}$			$(\frac{\Delta_1}{\Delta_i})^2$		
		$i=1$	$i=2$	$i=3$	$i=1$	$i=2$	$i=3$	$i=1$	$i=2$	$i=3$
1	$_{9}F^{19}$	0.71	0.66	0.53	0.18	0.21	0.33	1.00	0.73	0.30
2	$_{22}Ti^{47}$	0.51	0.49	0.43	0.21	0.23	0.25	1.00	0.80	0.64
3	$_{22}Ti^{48}$	0.65	0.58	0.42	0.17	0.20	0.28	1.00	0.64	0.36
4	$_{29}Cu^{65}$	0.77	0.66	0.50	0.12	0.18	0.27	1.00	0.43	0.30
5	$_{39}Y^{89}$	0.89	0.77	0.71	0.12	0.17	0.21	1.00	0.57	0.36
6	$_{45}Rh^{103}$	0.83	0.77	0.73	0.13	0.17	0.20	1.00	0.56	0.42
7	$_{46}Pd^{106}$	0.77	0.71	0.66	0.16	0.20	0.23	1.00	0.52	0.47
8	$_{46}Pd^{108}$	0.85	0.81	0.71	0.11	0.12	0.21	1.00	0.82	0.27
9	$_{47}Ag^{107}$	0.87	0.73	0.71	0.093	0.19	0.21	1.00	0.24	0.19
10	$_{47}Ag^{109}$	0.83	0.73	0.71	0.12	0.20	0.21	1.00	0.36	0.30
11	$_{49}In^{115}$	0.90	0.81	0.77	0.076	0.14	0.17	1.00	0.29	0.16
Averages		0.78	0.70	0.62	0.13	0.18	0.23	1.00	0.54	0.34

TABLE Id. The values of $f_i = \frac{R_{Th}}{R_{\exp}}$, $\frac{\Delta_i}{R_{\exp}} = \frac{1-f_1}{R_{\exp}}$, $(\frac{\Delta_1}{\Delta_i})^2$, and $(\frac{\Delta_2}{\Delta_i})^2$ for $i = 1$, $i = 2$, and $i = 3$ for four odd-odd and even-even nuclei, which are somewhat away from the general trend due to nuclear structural effects.

No.	Nucleus	$f_i = \frac{R_{Th}}{R_{\exp}}$			$\frac{\Delta_i}{R_{\exp}} = \frac{1-f_1}{R_{\exp}}$			$(\frac{\Delta_1}{\Delta_i})^2$			$(\frac{\Delta_2}{\Delta_i})^2$		
		$i=1$	$i=2$	$i=3$	$i=1$	$i=2$	$i=3$	$i=1$	$i=2$	$i=3$	$i=1$	$i=2$	$i=3$
1	$_{13}Al^{27}$	1.09	0.91	0.73	−0.071	+0.074	0.22	1.00	1.00	0.04	1.08	1.00	11.6
2	$_{15}P^{31}$	1.20	0.99	0.76	−0.17	0.009	0.21	1.00	343	0.64	0.0028	1.00	0.0018
3	$_{16}S^{32}$	1.40	1.10	0.85	−0.38	−0.097	0.14	1.00	444	0.73	0.067	1.00	0.47
4	$_{27}Co^{59}$	1.09	0.91	0.71	− 0.071	0.062	0.22	1.00	1.44	0.14	0.75	1.00	0.078

there is some systematics when we take $(\frac{\Delta_2}{\Delta_i})^2 = 1$ for $i = 2$. It seems to resemble the behavior of direct reaction as shown in Table IIc. These four cases therefore do not seem to represent the MSD reaction mechanism but the direct reaction.

This seems to indicate that for the eight even-even nuclei as shown in Table Ib, the incident particle creates two hole ($h = 2$, $p = 0$) configurations in the tightly bound ground levels of these even-even nuclei, whereas for some odd-even, odd-odd, and even-even target nuclei as given in Table Ic perhaps it involves other levels near the ground level of the target nuclei for the preequilibrium process, corresponding to $h = 1$, $p = 1$ and $h = 0$, $p = 2$, besides the dominant configuration $h = 2$, $p = 0$.

B.

We have calculated earlier [5] the values of $g_c^{Th}(\varepsilon_c)$ as a function of (ε_c) by calculating $g_{cn}^{Th}(\varepsilon_{cn})$ for the excitation of neutrons and ${g_{cp}}^{Th}(\varepsilon_{cp})$ for the excitation of protons, giving

$$g_c^{Th}(\varepsilon_c) = g_{cn}^{Th}(\varepsilon_{cn}) + g_{cp}^{Th}(\varepsilon_{cp})$$

described in detail in Ref. [5] from Eqs. (24a) to (26).

These calculations are based on Shlomo's theory as in Ref. [6] from Eq. (6) to Eq. (25). We have given in Table IIa, the details of these values. We have plotted $g_c^{Th}(\varepsilon)$ versus ε from $\varepsilon = -10$ to $\varepsilon = 80$ MeV in Fig. 3 where we have also indicated the experimental values of g_c(exp) and g_R(exp) at $\varepsilon = 14.8$ MeV and at $\varepsilon = -\varepsilon_f$, respectively. These values of g_c(exp) and g_R(exp) correspond to the spikes in Fig. 1.

It is evident that the experimental values of g_c(exp) and g_R(exp) are invariably much higher than the theoretical values. This is different from the comparison of experimental values of g_c(exp) for the 23 targets on the smooth portion (A) of Fig. 1 where it was possible to exactly match the experimental values of g_c(exp) with ε and obtain exact values of excitation energy $\langle\varepsilon_c\rangle$ as described in detail in Ref. [5] and given in Fig. 7 of that reference.

All the values of g_c(exp) and g_R(exp) have been obtained semiempirically by the hit and trial method to fit the experimental result of the energy spectra and the angular distribution as shown in Fig. 5 of Ref. [1] for V^{51} and Cu^{63} included among other nuclei. This is also the case for the other five nuclei, i.e., $_{22}Ti^{46}$, $_{24}Cr^{50}$, $_{24}Cr^{52}$, $_{26}Fe^{54}$, and $_{28}Ni^{60}$.

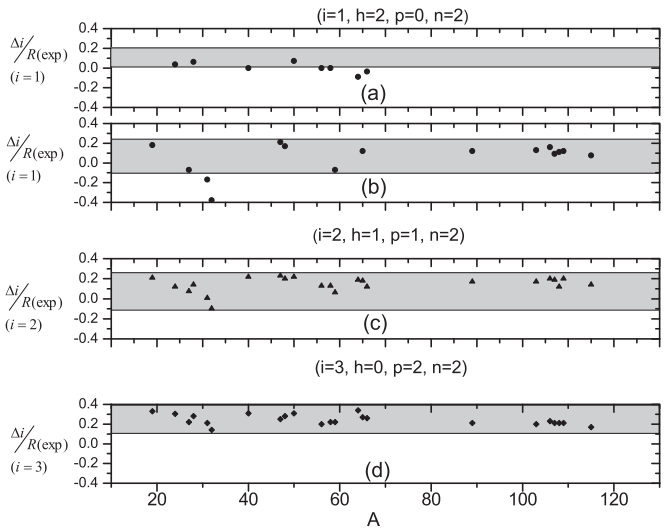

FIG. 2. The values of $\frac{\Delta_i}{R_{\exp}}$ (a) for eight even-even nuclei, (b) for even-odd, odd-odd, and even some even-even nuclei for $i = 1$, (c) for all targets for $i = 2$, and (d) for all targets for $i = 3$.

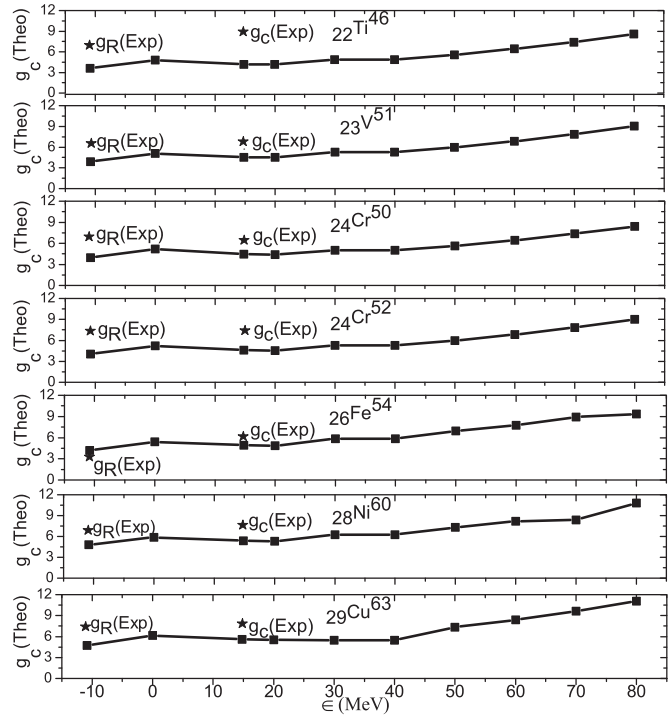

FIG. 3. The values of $g_c(Th)$ of the spikes as a function of incident energy ε for $_{22}Ti^{46}$, $_{23}V^{51}$, $_{24}Cr^{50}$, $_{24}Cr^{52}$, $_{26}Fe^{54}$, $_{28}Ni^{60}$, and $_{29}Cu^{63}$ along with g_c(exp) and g_R(exp).

TABLE IIa. The values of $g_c(Th)$ at different values of the excitation energy ε for the group of seven targets.

No.	Nucleus	ε_f	$\varepsilon = 0$	$\varepsilon = 14.8$ MeV	$\varepsilon = 20$ MeV	$\varepsilon = 30$ MeV	$\varepsilon = 40$ MeV	$\varepsilon = 50$ MeV	$\varepsilon = 60$ MeV	$\varepsilon = 70$ MeV	$\varepsilon = 80$ MeV
1	$_{22}Ti^{46}$	3.62(−10.74)	4.77	4.17	4.14	4.89	4.89	5.57	6.42	7.41	8.56
2	$_{23}V^{51}$	3.95(−10.83)	5.17	4.46	4.39	5.03	5.03	5.65	6.43	7.36	8.42
3	$_{24}Cr^{50}$	3.87(−10.29)	5.09	4.54	4.51	5.36	5.36	6.13	7.07	8.18	9.45
4	$_{24}Cr^{52}$	4.03(−10.91)	5.25	4.61	4.55	5.29	5.29	5.98	6.84	7.86	9.03
5	$_{26}Fe^{54}$	4.21(−10.83)	5.42	4.92	4.89	5.85	5.85	6.94	7.73	8.95	9.36
6	$_{28}Ni^{60}$	4.79(−10.33)	5.89	5.36	5.31	6.25	6.25	7.10	8.16	9.40	10.8
7	$_{29}Cu^{63}$	4.73(−10.32)	6.13	5.59	5.52	6.46	6.46	7.32	8.39	9.64	11.07

TABLE IIb. The values of $\varepsilon_C = E$, $\varepsilon_f = S$, V_0, $g_C(\text{exp}) = g_u(p)$, $g_R(\text{exp}) = g_0$, $\frac{g_C(\text{exp})}{g_R(\text{exp})} = R_{\text{exp}}$, and R_{Th} for $i = 1$, $i = 2$, and $i = 3$ configurations.

No.	Nucleus	$\varepsilon_C = E$	$\varepsilon_f = S$	V_0	$g_C(\text{exp}) = g_u(p)$	$g_R(\text{exp}) = g_0$	$\frac{g_C(\text{exp})}{g_R(\text{exp})} = R(\text{exp})$	R_{Th}(p,h) configuration		
								$h = 2\ p = 0$	$h = 1\ p = 1$	$h = 0\ p = 2$
1	$_{22}Ti^{46}$	56.4	34.26	41.6	9.21	6.79	1.3	1.4	0.73	0.8
2	$_{23}V^{51}$	56.5	34.7	41.7	6.91	6.48	1.07	1.24	1.17	0.85
3	$_{24}Cr^{50}$	56.5	34.01	41.7	6.48	6.48	1.00	1.4	1.2	0.88
4	$_{24}Cr^{52}$	56.0	34.09	41.8	8.00	7.45	1.07	1.4	1.15	0.86
5	$_{26}Fe^{54}$	56.5	34.77	41.8	6.00	3.45	1.13	1.3	1.13	0.86
6	$_{28}Ni^{60}$	56.0	34.47	41.2	8.00	6.97	1.15	1.36	1.12	0.88
7	$_{29}Cu^{63}$	56.0	33.68	41.0	8.00	7.51	1.06	1.49	1.12	0.87

TABLE IIc. The values of $f_i = \frac{R_{Th}}{R_{\text{exp}}}$, $\frac{\Delta_i}{R_{\text{exp}}} = \frac{1-f_1}{R_{\text{exp}}}$, and $(\frac{\Delta_1}{\Delta_i})^2$ for $i = 1$, $i = 2$, and $i = 3$ configurations.

No.	Nucleus	$f_i = \frac{R_{Th}}{R_{\text{exp}}}$			$\frac{\Delta_i}{R_{\text{exp}}} = \frac{1-f_1}{R_{\text{exp}}}$			$(\frac{\Delta_1}{\Delta_i})^2$		
		$i = 1$	$i = 2$	$i = 3$	$i = 1$	$i = 2$	$i = 3$	$i = 1$	$i = 2$	$i = 3$
1	$_{22}Ti^{46}$	1.07	0.66	0.77	−0.54	0.250	0.17	0.21	1.00	2.30
2	$_{23}V^{51}$	1.25	0.91	0.77	−0.23	0.075	0.21	0.10	1.00	0.12
3	$_{24}Cr^{50}$	1.40	1.2	0.88	−0.41	−0.020	0.12	0.25	1.00	1070
4	$_{24}Cr^{52}$	1.33	1.08	0.83	−0.32	0.075	0.12	0.13	1.00	0.39
5	$_{26}Fe^{54}$	1.17	1.02	0.77	−0.15	−0.018	0.20	0.014	1.00	0.21
6	$_{28}Ni^{60}$	1.20	0.91	0.70	−0.18	0.095	0.26	0.22	1.00	0.11
7	$_{29}Cu^{63}$	1.43	1.025	0.82	−0.40	−0.014	0.17	0.12	1.00	0.064

TABLE IIIa. The values of $g_T^{Th}(\varepsilon)$ at different values of the excitation energy ε for six target nuclei.

No.	Nucleus	ε_f	$\varepsilon = 0$	$\varepsilon = 14.8$ MeV	$\varepsilon = 20$ MeV	$\varepsilon = 30$ MeV	$\varepsilon = 40$ MeV	$\varepsilon = 50$ MeV	$\varepsilon = 60$ MeV	$\varepsilon = 70$ MeV	$\varepsilon = 80$ MeV
1	$_{40}Zr^{90}$	6.27(−12.92)	8.23	7.94	7.80	9.06	9.06	10.24	11.70	13.41	15.38
2	$_{42}Mo^{92}$	6.55(−13.31)	8.38	8.29	8.16	9.65	9.67	11.00	12.65	14.58	16.80
3	$_{41}Nb^{93}$	6.30(−12.40)	8.46	8.18	8.12	9.29	9.29	10.48	11.96	13.70	15.69
4	$_{42}Mo^{94}$	6.73(−12.13)	8.54	8.36	8.20	9.58	9.58	10.85	12.42	14.27	16.38
5	$_{42}Mo^{95}$	6.70(−12.40)	8.61	8.39	8.23	9.55	9.55	10.79	12.32	14.12	16.19
6	$_{42}Mo^{96}$	6.37(−13.51)	8.69	8.43	8.25	9.52	9.52	10.73	12.23	13.99	16.00

But so much deviation of g_c(exp) and g_R(exp) from values calculated using Shlomo's theory shows that Shlomo's model does not take into account certain features of the nuclear structure in the reaction mechanism. It is well known that theories of compound nucleus formation [7], direct reaction, and inelastic scattering [8], which were developed earlier, did not include the preequilibrium process for which the theory came much later and includes a formation of the compound process, through the MS, MSC processes, as well as evaporation, direct reaction, and inelastic scattering. The trial and error method of comparing experimental data with the Kalbach computer program automatically includes these processes.

On the other hand Shlomo's model, using the Green's function, does not seem to involve these nuclear structure effects. It is interesting that these seven nuclei in category B have high values of (ε_f), i.e., ≈34 MeV, compared to 30–32 MeV for most nuclei. These perhaps make the direct reaction more probable. It is interesting to note that for all these seven cases, the values of $\frac{g_c(\text{exp})}{g_R(\text{exp})}$ are much less than the values of the preequilibrium processes which is true for nuclei in category A. This ratio varies from 1.06 to 1.30 for these seven nuclei. On the other hand these values are 1.49, 1.33, and 1.37 for magic number nuclei, such as $_{20}Ca^{40}$, $_{28}Ni^{58}$, and $_{39}Y^{89}$ and vary from 1.025 to 1.83 for other nuclei in category A.

This shows that for category B nuclei, the direct knockout direct reaction process plays a significant role, which is not taken into account when one uses the Green's function approach while calculating the energy dependence by using Shlomo's model.

We have given in Table IIb, the values of $\langle\varepsilon_c\rangle$=$E$, (ε_f)=S, $\langle V_0\rangle$, $g_c(\text{exp}) = g_u(p)$, $g_R(\text{exp}) = g_o$, and $\frac{g_c(\text{exp})}{g_R(\text{exp})} = R_{\text{exp}}$ and R_{Th} for $i = 1, i = 2$, and $i = 3$ corresponding to $h = 2$, $p = 0$, $h = 1$, $p = 1$ and $h = 2$, $p = 0$, respectively, for the seven nuclear targets, plotted in Fig. 4 where we assumed $\langle\varepsilon_c\rangle \approx$ 56 MeV for all the targets. In Table IIc, we have given the values of $f_1 = \frac{R_{Th}}{R_{\text{exp}}}$, $\frac{\Delta_i}{R_{\text{exp}}} = \frac{1-f}{R_{\text{exp}}}$, and $(\frac{\Delta_2}{\Delta_i})^2$ for these nuclei for $i = 1$, $i = 2$, and $i = 3$. We have taken Δ_2 as the reference deviation because it gives the least deviation values as shown in the column for $\frac{\Delta_i}{R_{\text{exp}}}$ in Table IIc. We then, see that $(\frac{\Delta_2}{\Delta_i})^2$ for $(i = 1)$ and $(\frac{\Delta_2}{\Delta_i})^2$ for $(i = 3)$ have very small values, except for $_{22}Ti^{46}$ for $i = 2$ and $i = 3$.

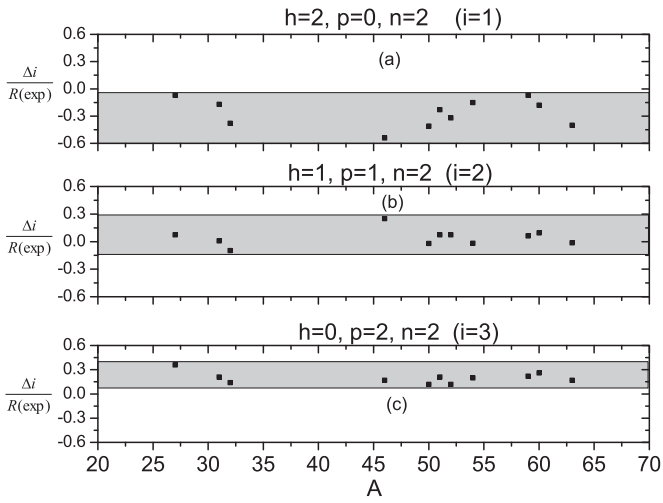

FIG. 4. The values of $\frac{\Delta_i}{R_{\text{exp}}}$ for three cases of (a) for seven cases of spikes for $i = 1$, (b) for seven cases of spikes for $i = 2$, and (c) for seven cases of spikes for $i = 3$.

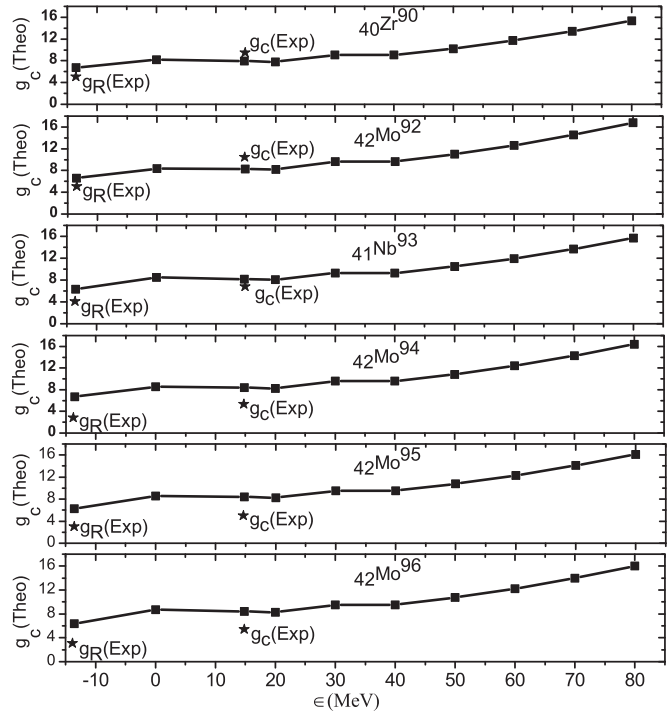

FIG. 5. The values of $g_c(Th)$ of dips as a function of incident energy for $_{40}Zr^{90}$, $_{42}Mo^{92}$, $_{41}Nb^{93}$, $_{42}Mo^{94}$, $_{42}Mo^{95}$, and $_{42}Mo^{96}$ along with g_c(exp) and g_R(exp).

This shows that these cases correspond to a direct reaction where not only the values of g_c(exp) and g_R(exp) are much larger than the theoretical values as calculated using Shlomo's model, showing that they do not correspond to the preequilibrium model, which accords with the $h = 2$, $p = 0$ $(i = 1)$ configuration as the prominent process, but on the other hand it accords with $h = 1$, $p = 1$ as the dominant configuration, corresponding to the direct reaction.

C.

The third category of target nuclei for which the behavior of the single-particle level densities g_c(exp) and g_R(exp) is different from the smooth curve A of Fig. 1 involves six target nuclei $_{40}Zr^{90}$, $_{42}Mo^{92}$, $_{41}Nb^{93}$, $_{42}Mo^{94}$, $_{42}Mo^{95}$, and $_{42}Mo^{96}$. For all these cases, the values of g_c(exp) are much lower than indicated for nuclei marked as A. All these nuclei contain quite close to the magic numbers of the neutrons, i.e., $n = 50, 53, 54$, etc. We have plotted in Fig. 5, and given in Table IIIa the values of $g_c^{Th}(\varepsilon_c)$ as a function of ε from $\varepsilon = -10$ to $\varepsilon = 80$ MeV along with g_c(exp) and g_R(exp) for these nuclei.

In general, the values of g_c(exp) and g_R(exp) for both these energies are much lower than the theoretically expected values except for $_{40}Zr^{90}$ and $_{42}Mo^{92}$ for which the values of g_c(exp)

TABLE IIIb. The values of $\varepsilon_C = E$, $\varepsilon_f = S$, V_0, $\frac{g_C(\exp)}{g_R(\exp)} = R(\exp)$, and R_{Th} for $i = 1$, $i = 2$, and $i = 3$, corresponding to $h = 2$, $p = 0$; $h = 1$, $p = 1$; and $h = 0$, $p = 2$ configurations.

No.	Nucleus	$\varepsilon_C = E$	$\varepsilon_f = S$	V_0	$g_C(\exp) = g_u(p)$	$g_R(\exp) = g_0$	$\frac{g_C(\exp)}{g_R(\exp)} = R(\exp)$	R_{Th}(p,h) configuration		
								$h = 2$ $p = 0$	$h = 1$ $p = 1$	$h = 0$ $p = 2$
1	$_{40}Zr^{90}$	40.0	32.38	40.2	8.97	4.97	1.80	1.13	1.09	0.95
2	$_{42}Mo^{92}$	40.0	31.97	39.6	10.48	4.97	2.10	1.14	1.04	0.94
3	$_{41}Nb^{93}$	40.0	32.6	40.2	6.98	4.08	1.62	1.13	1.04	0.95
4	$_{42}Mo^{94}$	40.0	32.87	40.2	5.45	2.97	1.8	1.03	1.04	0.95
5	$_{42}Mo^{95}$	40.0	32.60	39.5	5.45	2.97	1.8	1.03	1.04	0.95
6	$_{42}Mo^{96}$	40.0	31.49	39.5	5.33	2.91	1.84	1.15	1.05	0.95

are a little higher than the expected values in curve A at the 14.8 MeV energy of ε (both of them involve $N = 50$). Also the values of $g_R(\exp)$ are lower than the expected values for all cases.

We have given in Table IIIb, the values of $\langle\varepsilon_c\rangle = E$, $(\varepsilon_f) = S$, $\langle V_o\rangle$, $g_c(\exp)$, $g_R(\exp)$, $\frac{g_c(\exp)}{g_R(\exp)}$, and the values of R_{Th} for $i = 1$, $i = 2$, and $i = 3$, corresponding to $h = 2$, $p = 0$, $h = 1$, $p = 1$, $h = 0$, $p = 2$, respectively. In Fig. 6, we have plotted the values of $\frac{\Delta_i}{R_{\exp}}$ as a function of A for these six nuclei. Assuming $\langle\varepsilon_c\rangle$ as 40 MeV, we find that the values of $\frac{\Delta_i}{R_{\exp}}$ are nearly the same for the $h = 2$, $p = 0$ configuration as for the $h = 1$, $p = 1$ or the $h = 0$, $p = 2$ configurations.

It can be seen from Fig. 5 that if we extrapolate the values of $g_c(\exp)$ so that it crosses the theoretical values of $g_c^{Th}(\varepsilon_c)$ for $_{40}Zr^{90}$ and $_{42}Mo^{92}$ the energy of incidence comes out to be nearly zero. For $_{41}Nb^{93}$, it turns out to be nearly -14 MeV; for $_{42}Mo^{94}$, it is nearly -22 MeV, for $_{42}Mo^{95}$ again it is nearly -25 MeV, and for $_{42}Mo^{96}$ it is -18 MeV.

How should these results be interpreted?

It seems that the experimental values include the nuclear structure effect of the nuclei, which happen to have neutrons near the magic number 50, e.g., $_{40}Zr^{90}$ and $_{42}Mo^{92}$ have

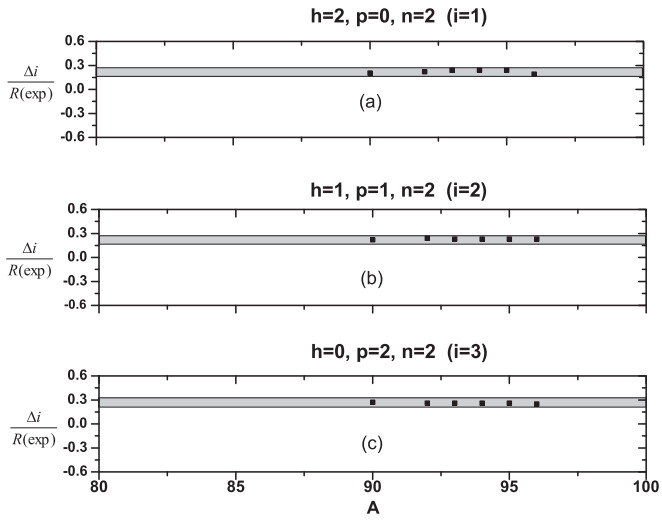

FIG. 6. The values of $\frac{\Delta_i}{R_{\exp}}$ for six cases of dips for (a) $i = 1$, (b) $i = 2$, and (c) $i = 3$.

50 neutrons, $_{41}Nb^{93}$ has 52 neutrons, $_{42}Mo^{94}$ has also 52 neutrons, $_{42}Mo^{95}$ has 53 neutrons, and $_{42}Mo^{96}$ has 54 neutrons. It is expected that $g_c(\exp)$ will be affected by these magic or near magic numbers due to the nuclear structural effects especially because of the binding energy of the ground state of these nuclei. Large binding energies and large Coulomb effect may not allow the protons to be excited to large positive energies. The large extrapolated negative energy of incidence, as referred to in the above paragraph, however may not be the realistic values of ε. The theoretical curve, based on Shlomo's theory, does not include the nuclear structure effect, and hence the large negative extrapolated values of ε do not seem to correspond to the real situation. This only indicates the effect of the large binding energies of the ground states of target nuclei.

Similarly the values of $g_R(\exp)$ as given in Table IIb when extrapolated yield large negative values for Fermi energies to hold well.

One may then assume that $g_c(\exp)$ and $g_R(\exp)$ correspond to MSD, the statistical process, whose values are expected to be low because of large binding energies of the ground states of these nuclei with magic or near magic numbers of neutrons. Quantum statistical fluctuation and MSD could be playing a role in determining the values of $g_c(\exp)$ and $g_R(\exp)$ and $\langle\varepsilon_c\rangle$ and (ε_f).

Although the values of $g_c(\exp)$ and $g_R(\exp)$ have been obtained by applying the Kalbach model to the experimental data by using the trial and error method, which will include the nuclear structure effects, the values of $\langle\varepsilon_c\rangle$ and (ε_f) correspond to the MSD process through quantum statistical fluctuations leading to a compound nucleus. The energy spectra for $_{40}Zr^{90}$, $_{42}Mo^{92}$, and $_{41}Nb^{93}$ have strong indications of compound nucleus formation as given in Fig. 4 of Ref. [1].

We assume that $\langle\varepsilon_c\rangle$ for these nuclei corresponds to ε_c close to the values for Y^{89}, Rh^{103}, Pd^{106}, etc. We therefore assume $\varepsilon_c = 0$ for all these nuclei so that according to Table IIc in Ref. [5] and Table Ia, $\langle\varepsilon_c\rangle \approx 40$ MeV.

We therefore give in Table IIIb the values of $\langle\varepsilon_c\rangle$ as $\approx$ 40 MeV corresponding to $\varepsilon = 0$ and take the Fermi energy values of $(\varepsilon_f) = S$. The values of $f_i = \frac{g_c^{Th}}{g_c(\exp)}$, $\frac{1-f_1}{R_{\exp}} = \frac{\Delta_i}{R_{\exp}}$, and $(\frac{\Delta_1}{\Delta_i})^2$ as given in Table IIIc are calculated on this basis. It is interesting to see that the values $\frac{\Delta_i}{R_{\exp}}$ and $(\frac{\Delta_1}{\Delta_i})^2$ for the three

TABLE IIIc. The values of $f_i = \frac{R_{Th}}{R_{\exp}}$, $\frac{\Delta_i}{R_{\exp}} = \frac{1-f_1}{R_{\exp}}$, and $(\frac{\Delta_2}{\Delta_i})^2$ for $i = 1$, $i = 2$, and $i = 3$.

No.	Nucleus	$f_i = \frac{R_{Th}}{R_{\exp}}$			$\frac{\Delta_i}{R_{\exp}} = \frac{1-f_1}{R_{\exp}}$			$(\frac{\Delta_1}{\Delta_i})^2$		
		$i = 1$	$i = 2$	$i = 3$	$i = 1$	$i = 2$	$i = 3$	$i = 1$	$i = 2$	$i = 3$
1	$_{40}Zr^{90}$	0.63	0.60	0.53	0.205	0.22	0.27	1.00	0.86	0.58
2	$_{42}Mo^{92}$	0.54	0.49	0.45	0.22	0.24	0.26	1.00	0.90	0.80
3	$_{41}Nb^{93}$	0.70	0.60	0.58	0.24	0.23	0.26	1.00	1.04	0.73
4	$_{42}Mo^{94}$	0.57	0.58	0.53	0.24	0.23	0.26	1.00	1.04	0.92
5	$_{42}Mo^{95}$	0.57	0.58	0.53	0.24	0.23	0.26	1.00	1.04	0.92
6	$_{42}Mo^{96}$	0.64	0.57	0.52	0.19	0.23	0.25	1.00	0.69	0.59

cases, i.e., $i = 1$, $i = 2$, and $i = 3$ do not differ too much from each other although $\frac{\Delta_i}{R_{\exp}}$ for $i = 1$ is the least. This could be the effect of the quantum statistical process.

III. CONCLUSION

Essentially one can summarize the results of this paper as follows:

(1) For category A target nuclei, both Kalbach's model and Shlomo's theory are applicable, and $h = 2$, $p = 0$ is the dominant configuration for the interaction as concluded in this paper, and the shell structures of $\langle \varepsilon_c \rangle$ as founded in Ref. [6] are consistent with each other. This supports the principle of the preequilibrium model of MSD and MSC for the nuclear reaction mechanism for these target nuclei for the (n, p) reaction at 14.8 MeV.

(2) On the other hand, for category B target nuclei, the Kalbach model creates values of $R_{\exp} = \frac{g_c\ (\exp)}{g_R\ (\exp)}$ which seem to support the knockout and nuclear-transfer-type direct reaction mechanisms with the dominance of the $h = 1$, $p = 1$ configuration due to low binding energies of nucleons in nuclear levels at the ground level in target nuclei. Shlomo's theory does not explain $g_c(\exp)$ and $g_R(\exp)$, which are much higher than the theoretical values given by Shlomo's theory. In other words $g_c(\exp)$ and $g_R(\exp)$ contain the effect of the direct reaction, but Shlomo's theory does not take into account the individual nuclear structure effects involved in the direct reaction.

(3) Similarly in the C category target nuclei, the values of $g_c(\exp)$ and $g_R(\exp)$ are much lower than that predicted by Shlomo's theory. This indicates that $g_c(\exp)$ and $g_R(\exp)$ contain the information for compound nucleus formation but with less contributions from the precompound process, which is given in Shlomo's theory. This is because of the effect of the nuclear structure due to the strong binding energy of the nucleons in the nuclear levels and the Coulomb effect in general. Perhaps quantum statistical fluctuations and the MSD process play a role in creating $g_c(\exp)$ and $g_R(\exp)$ at lower values and energies.

[1] G. Singh, H. S. Hans, T. S. Cheema, K. P. Singh, D. C. Tayal, J. Singh, and S. Ghosh, Phys. Rev. C **49**, 1066 (1994).

[2] C. Kalbach, Phys. Rev. C **23**, 124 (1981); **24**, 819 (1981), the PRECO-D2 program in calculating the preequlibrium and direct reaction double differential cross-sectional Los Alamos National Laboratory LA 10248-MS (1985).

[3] H. Feshbach, A. K. Kerman, and S. Koonin, Ann. Phys. (NY) **125**, 429 (1980).

[4] V. F. Weisskopf and D. H. Ewing, Phys. Rev. **57**, 472 (1940).

[5] H. S. Hans, G. Singh, A. Kumar, K. P. Singh, B. R. Behra, and S. Ghosh, Phys. Rev. C **85**, 054614 (2012).

[6] S. Shlomo, Nucl. Phys. A **539**, 17 (1992); Y. A. Bogila, V. H. Kolomietz, A. I. Samzahur, and S. Shlomo, Phys. Rev. C **53**, 855 (1996).

[7] N. Bohr, Nature (London) **137**, 344 (1936); J. M. Blatt and V. F. Weisskopf, *Theoretical Nuclear Physics* (Wiley, New York, 1952).

[8] E. O. Lawrence, E. M. Millan, and R. L. Thornton, Phys. Rev. **48**, 493 (1935); J. R. Oppenheimer and H. Phillips, *ibid.* **48**, 500 (1935).